





REACTIVE POWER COMPENSATION IN MEDIUM-VOLTAGE DISTRIBUTION NETWORKS THROUGH THYRISTOR-BASED SWITCHED COMPENSATORS AND THE ARTIFICIAL HUMMINGBIRD ALGORITHM

Compensación de potencia reactiva en redes de distribución de media tensión mediante compensadores conmutados basados en tiristores y el algoritmo de colibrí artificial

Dallany Giraldo-Aizales 
Universidad Distrital Francisco José de Caldas (Bogotá D.C., Colombia). 
dgiraldoa@udistrital.edu.co

Oscar-Danilo Montoya-Giraldo 
Universidad Distrital Francisco José de Caldas (Bogotá D.C., Colombia). 
odmontoyag@udistrital.edu.co

Walter Gil-González 
Universidad Tecnológica de Pereira (Pereira, Colombia). 
wjgil@utp.edu.co

Received: 30-09-2024

Accepted: 21-03-2025



ABSTRACT

This research addresses the optimal reactive power compensation problem in medium-voltage distribution networks by integrating Thyristor-based Switched Capacitors (TSCs) and applying the Artificial Hummingbird Algorithm (AHA). Using TSCs in distribution networks aims at reducing the annualized grid operating costs associated with energy losses while considering the costs of investment in reactive power compensators. The AHA—a bio-inspired metaheuristic optimization approach—is used to determine the optimal set of nodes and sizes for the TSCs. To estimate the expected annualized costs of energy losses, a classical power flow approach based on successive approximations is implemented, structured within a master-slave framework with the AHA. Numerical results on 33- and 69-bus systems demonstrate the effectiveness of the proposed approach compared to three other metaheuristic methods: the sine-cosine algorithm, the Chu & Beasley genetic algorithm, the particle swarm optimizer, and the black widow optimizer. All computational validations were performed using MATLAB software.

Keywords: annual operating costs minimization; artificial hummingbird algorithm; medium-voltage distribution networks; optimal reactive power compensation; thyristor-based switched capacitors.

RESUMEN

Esta investigación aborda el problema de la compensación óptima de potencia reactiva en redes de distribución de media tensión mediante la integración de compensadores conmutados basados en tiristores (TSCs) y la aplicación del algoritmo

artificial de colibrí (AHA). El uso de TSCs en redes de distribución busca reducir los costos operativos anualizados de la red que se relacionan con las pérdidas de energía, a la vez que se consideran los costos de inversión en compensadores de potencia reactiva. El AHA, un enfoque bioinspirado de optimización metaheurística, se utiliza para determinar el conjunto óptimo de nodos y tamaños para los TSCs. Para estimar los costos anualizados que se proyectan para las pérdidas de energía, se implementa un enfoque clásico de flujo de potencia basado en aproximaciones sucesivas, estructurado en el marco de una configuración maestro-esclavo con el AHA. Los resultados numéricos obtenidos en sistemas de 33 y 69 nodos demuestran la efectividad del enfoque propuesto del AHA en comparación con otros tres métodos metaheurísticos: el algoritmo seno-coseno, el algoritmo genético de Chu & Beasley, el optimizador de enjambre de partículas y el optimizador de viuda negra. Todas las validaciones computacionales se realizaron en el *software* MATLAB.

Palabras clave: algoritmo artificial del colibrí; compensación óptima de potencia reactiva; condensadores conmutados basados en tiristores; minimización de los costos operativos anuales; redes de distribución de media tensión.

COMPENSAÇÃO DE POTÊNCIA REATIVA EM REDES DE DISTRIBUIÇÃO DE MÉDIA TENSÃO POR MEIO DE COMPENSADORES COMUTADOS BASEADOS EM TIRISTORES E O ALGORITMO DO BEIJA-FLOR ARTIFICIAL

RESUMO

Esta pesquisa aborda o problema da compensação ótima de potência reativa em redes de distribuição de média tensão por meio da integração de compensadores comutados baseados em tiristores (TSCs) e a aplicação do algoritmo do beija-flor artificial (AHA). O uso de TSCs em redes de distribuição busca reduzir os custos operacionais anualizados da rede, relacionados às perdas de energia, considerando ao mesmo tempo os custos de investimento em compensadores de potência reativa. O AHA, uma abordagem bioinspirada de otimização meta-heurística, é utilizado para determinar o conjunto ótimo de nós e tamanhos para os TSCs. Para estimar os custos anualizados projetados para as perdas de energia, é implementada uma abordagem clássica de fluxo de potência baseada em aproximações sucessivas, estruturada no contexto de uma configuração mestre-esclavo com o AHA. Os resultados numéricos obtidos em sistemas de 33 e 69 nós demonstram a eficácia da abordagem proposta pelo AHA em comparação com outros três métodos meta-heurísticos: o algoritmo seno-cosseno, o algoritmo genético de Chu & Beasley, o otimizador de enxame de partículas e o otimizador de viúva-negra. Todas as validações computacionais foram realizadas no *software* MATLAB.

Palavras-chave: algoritmo do beija-flor artificial; compensadores comutados baseados em tiristores; compensação ótima de potência reativa; minimização dos custos operacionais anuais; redes de distribuição de média tensão.

Parameters

C_{kWh}	Expected annual costs of energy losses
T	Total days in an ordinary year
Y_{km}	Admittance magnitude relating nodes k and m
φ_{km}	Admittance angle related nodes k and m
ω_1	Cubic constant associated with investments in TSC devices
ω_2	Quadratic constant associated with investments in TSC devices
ω_3	Linear constant associated with investments in TSC devices
k_1, k_2	Annualization factors regarding investments in TSC devices
Δh	Period under analysis
I_{km}^{max}	Current limitations of the conductor connecting nodes k and m

V_{\min}, V_{\max}	Minimum and maximum voltage bounds
q_{\max}	Maximum size permitted for a single TSC connected to a bus k
X_{\max}^{TSC}	Maximum number of TSCs available for installation
ρ_{\max}^{TSC}	Maximum tolerance error
Y_{ds}	Complex nodal admittance matrix of the network that relates the demand nodes and the substation node
Y_{dd}	Complex nodal admittance matrix of the network that relates the demand nodes to each other
n_p	Total number of individuals in the population
n_v	Total number of variables
β	Guiding factor
FP	Flight pattern vector
X_{\min}, X_{\max}	Upper and lower bounds for the AHA decision variables vector

Sets and indices

N	Set of network nodes
H	Set of daily periods
k,m	Node subscript in the network
h	Time subscript for daily periods
s	Subscript related to the substation bus in the network
d	Subscript related to the demand nodes in the network
p	Individuals in the AHA population
v	Position of the AHA vector variable
i	Subscript related to hummingbirds
t	Subscript related to the iteration of the AHA

Variables

f	
f_1	Annual operating costs regarding energy losses
f_2	Expected investment costs
q_k^{TSC}	Rated power of the TSC installed at node k
v_{kh}	Voltage magnitude at node k in period h
θ_{kh}	Voltage angle at node k in period h
i_{kmh}^r, i_{kmh}^i	Real and imaginary parts of the complex current flow between nodes k and m
p_{kh}^g, q_{kh}^g	Active and reactive generation at node k in period h
p_{kh}^d, q_{kh}^d	Active and reactive demand at node k in period h
q_{kh}^{TSC}	Reactive power injected by the TSC at node k in period h

x_k	Binary variable for TSC installation at node k
μ	Random vector with a uniform distribution
x_{worst}	Worst food source of the AHA
$V_i(t + 1)$	Next position of the hummingbird i
X_i	Current position of the hummingbird i

1. INTRODUCTION

Reactive power compensation in Medium-Voltage Distribution Networks (MVDNs) is a proven technique widely used by distribution companies to minimize power losses and improve voltage profiles in electrical grids, particularly those characterized by resistive-inductive loads [1]. This method involves integrating capacitor-based devices that inject the necessary reactive power into the grid, thus adapting to varying demand profiles. Traditionally, reactive power compensation has relied on fixed, or variable-step capacitor banks strategically placed along the feeder. While this approach offers advantages, injecting fixed blocks of reactive power may not adequately address the dynamic nature of active and reactive power demands. In this vein, a more precise solution involves the installation of Flexible Alternating Current Transmission Systems (FACTS), such as static VAR compensators (SVCs), Static Synchronous Compensators (STATCOMs), and Thyristor-Switched Capacitors (TSCs). TSCs offer several advantages over static SVCs and STATCOMs in some contexts [2]. TSCs have a lower initial cost thanks to their simpler design and the absence of complex power electronic components, which makes them more economical in terms of capital investment. Additionally, TSCs can be more efficient in terms of energy losses, particularly in scenarios that require reactive power compensation. Moreover, TSCs tend to have a longer lifespan and require less maintenance due to their straightforward design [3].

The optimal location and sizing of FACTS in power systems have been thoroughly examined in specialized literature. By means of the particle swarm optimization (PSO) algorithm, the study by [4] optimized the placement of FACTS in the IEEE 39-bus system while considering the impact of electric vehicles. Furthermore, [5] employed the seeker optimization algorithm to install TSCs in the IEEE 30-bus system, identifying their optimal location and size. This approach enhanced the transmission system's capacity and voltage profile while reducing the associated costs. For the optimal integration of FACTS into distribution systems, the work by [6] proposed a hybrid approach combining fuzzy multi-objective optimization and ant colony algorithms. This method aimed to optimize the simultaneous reconfiguration and placement of solar energy generation and FACTS, reducing energy losses and improving voltage profiles by considering their combined impact.

The study by [7] introduced a heuristic technique that utilizes power losses and voltage indices to determine the optimal placement and sizing of FACTS in electrical distribution systems. This method was evaluated using the IEEE 33-bus test system, focusing solely on maximum load conditions. Additionally, [8] presented an approach combining analytical and heuristic optimization techniques to find the optimal location and size of FACTS. This work also discusses common objective functions in this field (e.g., indicators for voltage stability and power losses).

Furthermore, [9] used a multi-objective PSO algorithm for optimal siting and sizing of FACTS while considering the reconfiguration of the electrical distribution network. The multi-objective function included minimizing active energy losses, improving the voltage stability index, and reducing the load capacity factor of the distribution lines. However, this approach had some limitations; it only considered optimization under maximum load conditions.

Notably, most of the previous works have not considered the installation of TSCs in distribution systems, which offer advantages over SVCs and D-STATCOMs. In this vein, this paper presents a methodology for addressing the optimal siting and sizing of TSCs in MVDNs to minimize the expected grid operating costs associated with energy losses while considering the annualized investments in these devices. The methodology involves two stages: a master stage and a slave stage.

In the leader stage, the artificial hummingbird algorithm (AHA) is employed to determine the optimal placement and size of TSCs for reactive power compensation in MVDNs. In the follower stage, a power flow analysis is conducted using the successive approximations method. The effectiveness of the proposed methodology was evaluated in a 33-bus test system, it demonstrated superior results compared to other metaheuristic algorithms.

The remainder of this research is structured as follows. Section II describes the solution methodology, which includes the mathematical model for the optimal siting and sizing of TSCs in distribution networks, with the purpose of minimizing investment and operating costs, and the solution strategy, which is based on a hybridization of the AHA approach with the successive approximations power flow method within a master-slave optimization framework. The master stage is entrusted with defining the locations and sizes of the TSCs, while the slave stage evaluates the technical performance of the solution's operating costs regarding energy losses. Section III outlines the main characteristics of the test feeders analyzed, which are composed of 33 and 69 nodes operating with a line-to-ground voltage equivalent to 12.66 kV and a radial structure. This section also presents, analyzes, and discusses the main numerical results in contrast with previous literature reports. Finally, Section IV presents the main concluding remarks derived from this research, as well as some possible future work.

2. METHODOLOGY

To solve the problem regarding the optimal location and sizing of TSCs in distribution networks, two main elements are considered: the formulation of the problem and its master-slave optimization approach, which will define the optimal locations and sizes of the TSCs and evaluate the technical feasibility of each device combination. These elements are detailed below.

A. Mathematical Formulation

The mathematical formulation for the studied problem can be categorized as a mixed-integer nonlinear programming (MINLP) model. Its integer variables correspond to the selection of nodes for the installation of reactive power compensators, while its continuous variables relate to the power flow equations [10].

1) Objective Function. The effective integration of TSCs is an economic optimization problem, as the main idea of connecting and operating reactive power compensators in MVDNs is to minimize the expected energy losses and annualized TSC investment costs [1]. This objective function is formulated below:

$$f = f_1 + f_2 \quad (1)$$

$$f_1 = c_{kWh} T \sum h \sum k \sum m v_{kh} v_{mh} Y_{km} \cos \cos(\theta_{kh} - \theta_{mh} - \varphi_{km}) \Delta h \quad (2)$$

$$f_2 = T \left(\frac{k_1}{k_2} \right) \sum k q_k^{\text{TSC}} \left(\omega_1 q_k^{\text{TSC}^2} + \omega_2 q_k^{\text{TSC}} + \omega_3 \right) \quad (3)$$

where the annual operating costs regarding energy losses are denoted by f_1 ; the expected TSC investment costs are represented by f_2 ; C_{kWh} is a constant associated with the expected annual costs of energy losses; T denotes the total days in an ordinary year (i.e., 365 days); v_{kh} and v_{mh} define the expected voltage magnitudes at buses k and m during period h , which have angular values defined by θ_{kh} and θ_{mh} , respectively; the magnitude and angle of the admittance relating nodes k and m are determined by Y_{km} and φ_{km} , while Δh determines the daily time interval, typically one hour or fractions of hour; the variable q_k^{TSC} represents the expected size of the TSC connected to bus k ; coefficients ω_1 , ω_2 , and ω_3 represent the cubic, quadratic, and linear constants associated with investments in TSCs; and k_1 and k_2 are constants associated with the annual investment costs over a ten-year planning horizon [10]. Note that N is the set containing all the network nodes, and H is the set containing all the daily time intervals.

2) Constraints. The optimal integration of TSCs in MVDNs demands several important considerations. These include ensuring the nodal active and reactive power balance, adhering to limitations on the maximum and minimum current flow for the distribution lines, maintaining voltage regulation within specified boundaries, determining the appropriate number of TSCs for installation, and accounting for their capacity to inject or absorb reactive power, among other factors [1]. The set of constraints associated with the problem under study are described below:

- **Power Equilibrium.** The equations for nodal power balance at node , which address both active and reactive power, involve adding up the generated or demanded power. These sums are then equated to the injected power flow, whether active or reactive [1]. By applying the nodal voltage formulation method, these constraints can be represented as follows:

$$p_{kh}^g - p_{kh}^d = \sum_{k \in N} \sum_{m \in N} v_{kh} v_{mh} Y_{km} \cos \cos(\theta_{kh} - \theta_{mh} - \varphi_{km}) \Delta h \quad \{\forall k \in N \quad \forall h \in H\} \quad (4)$$

$$q_{kh}^g - q_{kh}^d + q_{kh}^{\text{TSC}} = \sum_{k \in N} \sum_{m \in N} v_{kh} v_{mh} Y_{km} \sin \sin(\theta_{kh} - \theta_{mh} - \varphi_{km}) \Delta h, \quad \{\forall k \in N \quad \forall h \in H\} \quad (5)$$

where p_{kh}^g and q_{kh}^g represent the active and reactive power generation values at the substation node connected to bus k in period h ; p_{kh}^d and q_{kh}^d are the active and reactive power consumption at node k during period h , respectively; and q_{kh}^{TSC} denotes the reactive power injection at bus k .

- **Current Flow Calculations.** To ensure that the current flowing through all the distribution lines does not exceed the thermal limitations of the installed distribution wires [11], the following constraints are considered. These are obtained using the real and imaginary part of the complex current flow, i.e., $I_{kmh} = i_{kmh}^r + j i_{kmh}^i$.

$$i_{kmh}^r = y_{km} (v_{kh} \cos(\theta_{kh} - \varphi_{km}) - v_{mh} \cos(\theta_{mh} - \varphi_{km})) \quad \{\forall km \in L \quad \forall h \in H\} \quad (6)$$

$$i_{kmh}^i = y_{km} (v_{kh} \sin(\theta_{kh} - \varphi_{km}) - v_{mh} \sin(\theta_{mh} - \varphi_{km})) \quad \{\forall km \in L \quad \forall h \in H\} \quad (7)$$

$$\sqrt{i_{kmh}^r{}^2 + i_{kmh}^i{}^2} \leq i_{km}^{\max} \quad \{\forall km \in L \quad \forall h \in H\} \quad (8)$$

where y_{km} represents the magnitude of the admittance associated with the distribution line connecting nodes k and m , which has an angle defined by φ_{km} ; and i_{km}^{\max} is the thermal current limit applicable to the conductor installed in the route connecting nodes k and m . Note that L is the set that contains all the distribution branches.

- **Grid Operating Conditions.** To ensure a correct network operation, typically under steady-state conditions, regulatory entities require that all load nodes observe maximum and minimum voltage bounds [12] with respect to the nominal network voltage at the terminals of the substation. These constraints are listed below.

$$v_{sh} = V_{\text{nom}}, \theta_{sh} = 0 \quad (s = \text{substation bus} \quad \forall h \in H) \quad (9)$$

$$V_{\min} \leq v_{kh} \leq V_{\max} \quad \{\forall k \in N \quad \forall h \in H\} \quad (10)$$

where v_{sh} represents the voltage variable at the terminals of the substation, θ_{sh} is its angular phase per period, and V_{nom} denotes the line-to-ground voltage of the distribution network.

- **Location and sizing of TSCs.** The analysis of TSCs in distribution networks requires knowing two main characteristics: location (binary variable) and size (continuous variable) [1]. In addition, the expected daily operation behavior of these devices must be defined. All these constraints are defined below:

$$0 \leq q_k^{\text{TSC}} \leq x_k q_{\max}^{\text{TSC}} \quad \forall k \in N \quad (11)$$

$$-q_k^{\text{TSC}} \leq q_{kh}^{\text{TSC}} \leq q_k^{\text{TSC}} \quad \{\forall k \in N \quad \forall h \in H\} \quad (12)$$

$$\sum_{k \in N} x_k \leq x_{\max}^{\text{TSC}} \quad (13)$$

where q_{\max}^{TSC} represents the maximum size permitted for a single TSC connected to bus k , whose location is defined by the activation of the binary variable x_k ; and x_{\max}^{TSC} is a constant parameter defining all the TSCs available for installation.

Remark 1

The optimization model defined from (1) to (13) belongs to the family of nonlinear non-convex MINLP models due to the combination of binary and continuous variables with nonlinear functions and constraints. To solve these models, literature reports the application of hybrid optimization strategies based on metaheuristics and numerical methods, with excellent numerical performance and adequate computation time requirements [1].

B. Solution Methodology

To address the studied problem, this research proposes a master-slave optimization approach. At the master stage, the AHA is employed to determine the expected sizes and locations of the TSCs, i.e., the values for the variables q_k^{TSC} and x_k . The information on the expected sizes is transferred to the slave stage, which employs a classical power flow approach entrusted with solving the power equilibrium constraints to evaluate the technical feasibility of the solution, as shown below.

1) Slave Stage: The Successive Approximations Power Flow Method. When implementing metaheuristic optimization methodologies applicable to electrical networks that consider power equilibrium constraints, as shown in Equations (4) and (5), a numerical solution is always required [13]. To solve these equations, multiple methods have been reported in the specialized literature [14]. In this research, as recommended by the authors of [1], the successive approximations power flow method is used at the slave stage, as it offers convergence guarantees and an easy computational implementation via a complex variable-domain formulation. The equations used for the computational implementation of the successive approximations power flow method are:

$$V_{dh}^{m+1} = -Y_{dd}^{-1} \left(\text{diag}^{-1} \left(V_{dh}^{m*} \right) S_{dh} \left(x, q_h^{TSC} \right) + Y_{ds} V_{sh} \right) \quad \forall h \in H \quad (14)$$

$$\max_m \left\{ \left| V_{dh}^{m+1} \right| - \left| V_{dh}^m \right| \right\} \leq \rho_{\max} \quad \forall h \in H \quad (15)$$

where V_{dh}^{m+1} is the vector containing all the voltage variables in the complex domain during the iteration $m+1$, with m being the iteration counter; V_{sh} denotes the vector containing the voltage profile at the terminals of the substation bus per period of study; Y_{ds} and Y_{dd} represent two subcomponents of the network's nodal admittance matrix that relate the demand nodes to the substation node and to each other; $S_{dh}(x, q_h^{TSC})$ is a vector containing the entirety of the complex demand consumption per period of analysis and including the effect of reactive power injection on all the TSCs installed along the distribution grid; the function $\max_m \{ \cdot \}$ determines the maximum value of the argument, and ρ_{\max} is the maximum tolerance error permitted during the power flow solution.

Equations (14) and (15) represent the complex-domain variable representation of the power flow problem in electrical distribution networks via the successive approximations power flow method [15].

Remark 2

The solution to the power flow problem, i.e., the recursive evaluation of the Power Flow Formula (13) until the convergence criterion is met, as shown in (14), provides the solutions for the nodal voltages in and allows evaluating the expected costs of energy losses, as denoted by in Equation (2), for each possible combination of TSC locations and sizes the master stage.

2) Master Stage: The Artificial Hummingbird Algorithm. The AHA is a nature-inspired optimization technique modeled after the foraging and hovering behavior of hummingbirds. It aims to solve complex optimization problems by mimicking the agile flight patterns and efficient search strategies of these birds as they look for nectar [16, 17]. The algorithm incorporates mechanisms for the exploration and exploitation of the search space, allowing it to effectively balance global and local search capabilities [18, 19]. The AHA is promising in various applications due to its ability to efficiently find high-quality solutions in complex and dynamic environments.

- **Encoding and Initial Population.** The implementation of population-based metaheuristic optimizers requires an encoding that allows representing the decision variables of interest. In our case, the AHA is used to determine the location and size of the TSCs to be installed in the distribution network. In this context, a discrete-continuous encoding is proposed, as shown in Table 1.

Table 1. Proposed problem encoding using a discrete-continuous representation.

	Nodal location		Sizes (Mvar)		
10	k	25	0.1258	0.2585	0.5632

In the proposed encoding, note that:

The activated binary variables are $x_{10} = 1$, $X_k = 1$, and $x_{25} = 1$.

The assigned sizes for the TSCs connected to these nodes are $q_{10}^{\text{TSC}} = 0.1258$, $q_k^{\text{TSC}} = 0.2585$, and $q_{25}^{\text{TSC}} = 0.5632$ Mvar.

This encoding is a combination of integer numbers associated with the total number of nodes in the grid and a subset of real numbers related to the expected sizes of the TSCs.

Remark 3

This encoding (Figure 1) belongs to the family of discrete-continuous problem representations, as proposed by CITATION SantamariaHenao2023 \l 9226 [1]. Its main advantage is that the Set of Constraints (11)-(13) is directly satisfied during the optimization process.

To explore and exploit the solution space, the AHA approach uses an initial population of size $n_s \times n_v$, where n_s represents the number of individuals in the population, i.e., the number of hummingbirds, and the number of variables, i.e., two times the number of TSCs available for installation. Equation (16) defines the general structure of the population [17].

$$P = \left[x_{11} \cdots x_{1np} \quad \vdots \quad \vdots \quad x_{ns1} \cdots x_{nps} \right] \quad (16)$$

In addition, the AHA implementation requires defining a vector that contains the objective function value or its equivalent (F) and the visit table (VT) [17]. These are defined in Equations (17) and (18).

$$F = \left[f_1, \vdots, f_{ns} \right] \quad (17)$$

$$VT_{(a,b)} = \left\{ 0 \quad a \neq b, \text{null} \quad a = b, \quad a, b = 1, 2, \dots, n_s \right\} \quad (18)$$

- **Guided Foraging.** In this approach, each hummingbird selects its target food source based on two key factors: the nectar-refilling rate and the visit level. The guided foraging process is carried out as follows [17], by defining the next position :

$$v_i(t+1) = x_{i,TP}(t) + \beta \times FP \times (x_i(t) - x_{i,TP}(t)) \quad (19)$$

where $X_i(t)$ defines the location of the i -th food source at iteration t . The location of the target food that the i -th hummingbird will visit is defined by $X_{i,TP}(t)$. In addition, β is the guiding factor, which is acquired using normal distribution. FP is the flight pattern vector. The location of the i -th food source is updated using Equation (20).

$$x_i(t+1) = \{v_i(t+1) \quad f(x_i(t)) > f(v_i(t+1)), x_i(t) \quad \text{otherwise}\} \quad (20)$$

- **Territorial foraging.** After consuming nectar from a flower, a hummingbird seeks out new food sources. One effective strategy for the hummingbird is to move to a neighboring area, where it may discover additional resources. This behavior is mathematically represented by Equation (21). Here, the parameter represents the territorial factor, which is derived from a normal distribution [17].

$$v_i(t+1) = x_i(t) + \varepsilon \times FP \times x_i(t) \quad (21)$$

- **Migration Foraging.** This foraging strategy is based on randomness. Hummingbirds do not always know where the best places to find food are, so they must explore new regions randomly. This can lead to the discovery of new food sources. The migration of the hummingbird can be expressed as follows [20]:

$$x_{\text{worst}}(t+1) = x_{\text{min}} + \mu \times (x_{\text{max}} - x_{\text{min}}) \quad (22)$$

where μ is a vector randomly generated with a uniform distribution; x_{max} and x_{min} represent the upper and lower bounds applicable to the vector of decision variables; and x_{worst} defines the worst food source.

Remark 4

The AHA evolves from an initial population based on (19) to (22) and the local and global exploitation and exploration rules. However, its performance depends on the programmer's ability to implement said rules and their expert knowledge of the studied optimization problem.

3. RESULTS AND DISCUSSIONS

This section presents the test feeders used to validate our approach, which consist of 33 and 69 nodes [21], as well as the numerical results obtained and their corresponding analysis and discussions.

A. Test Feeders

The analyzed MVDNs feature 33 and 66 nodes and a radial topology. The nominal voltage at the substation terminals of both test feeders is 12.66 kV [1]. The electrical information on these systems is listed in Tables 2 and 3.

Table 2. Electrical information for the 33-bus grid.

Node K	Node m	R_{km} (Ω)	X_{km} (Ω)	P_m^d (kW)	Q_m^d (kvar)	Node K	Node m	R_{km} (Ω)	X_{km} (Ω)	P_m^d (kW)	Q_m^d (kvar)
1	2	0.0922	0.0477	100	60	17	18	0.7320	0.5740	90	40
2	3	0.4930	0.2511	90	40	2	19	0.1640	0.1565	90	40
3	4	0.3660	0.1864	120	80	19	20	1.5042	1.3554	90	40
4	5	0.3811	0.1941	60	30	20	21	0.4095	0.4784	90	40
5	6	0.8190	0.7070	60	20	21	22	0.7089	0.9373	90	40
6	7	0.1872	0.6188	200	100	3	23	0.4512	0.3083	90	50
7	8	1.7114	1.2351	200	100	23	24	0.8980	0.7091	420	200
8	9	1.0300	0.7400	60	20	24	25	0.8960	0.7011	420	200
9	10	1.0400	0.7400	60	20	6	26	0.2030	0.1034	60	25
10	11	0.1966	0.0650	45	30	26	27	0.2842	0.1447	60	25
11	12	0.3744	0.1238	60	35	27	28	1.0590	0.9337	60	20
12	13	1.4680	1.1550	60	35	28	29	0.8042	0.7006	120	70
13	14	0.5416	0.7129	120	80	29	30	0.5075	0.2585	200	600
14	15	0.5910	0.5260	60	10	30	31	0.9744	0.9630	150	70
15	16	0.7463	0.5450	60	20	31	32	0.3105	0.3619	210	100
16	17	1.2860	1.7210	60	20	32	33	0.3410	0.5302	60	40

Table 3. Electrical information for the 69-bus grid.

Node K	Node m	R_{km} (Ω)	X_{km} (Ω)	P_m^d (kW)	Q_m^d (kvar)	Node K	Node m	R_{km} (Ω)	X_{km} (Ω)	P_m^d (kW)	Q_m^d (kvar)
1	2	0.0005	0.0012	0.00	0.00	3	36	0.0044	0.0108	26.00	18.55
2	3	0.0005	0.0012	0.00	0.00	36	37	0.0640	0.1565	26.00	18.55
3	4	0.0015	0.0036	0.00	0.00	37	38	0.1053	0.1230	0.00	0.00
4	5	0.0251	0.0294	0.00	0.00	38	39	0.0304	0.0355	24.00	17.00
5	6	0.3660	0.1864	2.60	2.20	39	40	0.0018	0.0021	24.00	17.00
6	7	0.3810	0.1941	40.40	30.00	40	41	0.7283	0.8509	1.20	1.00
7	8	0.0922	0.0470	75.00	54.00	41	42	0.3100	0.3623	0.00	0.00
8	9	0.0493	0.0251	30.00	22.00	42	43	0.0410	0.0478	6.00	4.30
9	10	0.8190	0.2707	28.00	19.00	43	44	0.0092	0.0116	0.00	0.00
10	11	0.1872	0.0619	145.00	104.00	44	45	0.1089	0.1373	39.22	26.30
11	12	0.7114	0.2351	145.00	104.00	45	46	0.0009	0.0012	29.22	26.30
12	13	10.300	0.3400	8.00	5.00	4	47	0.0034	0.0084	0.00	0.00
13	14	10.440	0.3450	8.00	5.50	47	48	0.0851	0.2083	79.00	56.40
14	15	10.580	0.3496	0.00	0.00	48	49	0.2898	0.7091	384.70	274.50
15	16	0.1966	0.0650	45.50	30.00	49	50	0.0822	0.2011	384.70	274.50
16	17	0.3744	0.1238	60.00	35.00	8	51	0.0928	0.0473	40.50	28.30
17	18	0.0047	0.0016	60.00	35.00	51	52	0.3319	0.1114	3.60	2.70
18	19	0.3276	0.1083	0.00	0.00	9	53	0.1740	0.0886	4.35	3.50
19	20	0.2106	0.0690	1.00	0.60	53	54	0.2030	0.1034	26.40	19.00
20	21	0.3416	0.1129	114.00	81.00	54	55	0.2842	0.1447	24.00	17.20
21	22	0.0140	0.0046	5.00	3.50	55	56	0.2813	0.1433	0.00	0.00
22	23	0.1591	0.0526	0.00	0.00	56	57	15.900	0.5337	0.00	0.00
23	24	0.3463	0.1145	28.00	20.00	57	58	0.7837	0.2630	0.00	0.00
24	25	0.7488	0.2475	0.00	0.00	58	59	0.3042	0.1006	100.00	72.00
25	26	0.3089	0.1021	14.00	10.00	59	60	0.3861	0.1172	0.00	0.00
26	27	0.1732	0.0572	14.00	10.00	60	61	0.5075	0.2585	1244.00	888.00
3	28	0.0044	0.0108	26.00	18.60	61	62	0.0974	0.0496	32.00	23.00
28	29	0.0640	0.1565	26.00	18.60	62	63	0.1450	0.0738	0.00	0.00
29	30	0.3978	0.1315	0.00	0.00	63	64	0.7105	0.3619	227.00	162.00
30	31	0.0702	0.0232	0.00	0.00	64	65	10.410	0.5302	59.00	42.00
31	32	0.3510	0.1160	0.00	0.00	11	66	0.2012	0.0611	18.00	13.00
32	33	0.8390	0.2816	14.00	10.00	66	67	0.0470	0.0140	18.00	13.00
33	34	17.080	0.5646	19.50	14.00	12	68	0.7394	0.2444	28.00	20.00
34	35	14.740	0.4873	6.00	4.00	68	69	0.0047	0.0016	28.00	20.00

B. Daily Operation Curves and TSC Parameters

To evaluate the performance of the TSCs installed in both test feeders, the peak power consumption per node (Tables 2 and 3) is multiplied by the percent power consumption reported (Table 4) for each period.

Table 4. Daily active and reactive power consumptions measured every 30 minutes.

Period (h)	Active power (%)	Reactive power (%)	Period (h)	Active power (%)	Reactive power (%)
1	0.3400	0.2954	25	0.9400	0.6764
2	0.2800	0.2238	26	0.9400	0.7228
3	0.2200	0.1964	27	0.9000	0.7754
4	0.2200	0.1666	28	0.8400	0.6868
5	0.2200	0.1478	29	0.8600	0.7542
6	0.2000	0.1654	30	0.9000	0.8538
7	0.1800	0.1662	31	0.9000	0.8448
8	0.1800	0.1274	32	0.9000	0.7294
9	0.1800	0.1404	33	0.9000	0.8452
10	0.2000	0.1750	34	0.9000	0.6162
11	0.2200	0.1456	35	0.9000	0.5988
12	0.2600	0.2428	36	0.9000	0.6672
13	0.2800	0.2462	37	0.8600	0.7086
14	0.3400	0.2780	38	0.8400	0.6798
15	0.4000	0.2820	39	0.9200	0.8468
16	0.5000	0.3996	40	1.0000	0.8122
17	0.6200	0.4994	41	0.9800	0.7640
18	0.6800	0.6448	42	0.9400	0.7640
19	0.7200	0.6526	43	0.9000	0.7774
20	0.7800	0.7322	44	0.8400	0.5502
21	0.8400	0.7170	45	0.7600	0.6766
22	0.8600	0.6632	46	0.6800	0.4710
23	0.9000	0.8374	47	0.5800	0.4602
24	0.9200	0.7304	48	0.5000	0.3636

In addition, the TSC parameters regarding the expected operating costs are listed in [Table 5](#). This information was adapted from [1].

Table 5. Parameterization of f_2 (investment in TSCs)

Parameter	Value	Unit	Parameter	Value	Unit
ω_1	1.50	USD/Mvar ³	ω_2	-713.00	USD/Mvar ²
ω_2	153750	USD/Mvar	T	365	Days
k_1	6/2190	1/day	k_2	10	Years
Δ_h	1/2	hour	C_{kWh}	0.1390	kWh/day

4. DISCUSSION

This section presents, analyzes, and discusses the numerical simulations carried out for each test feeder. Results include the optimal locations and sizes of the TSCs, the expected annual investment and

operating costs, and the expected grid improvements after 100 consecutive executions of the solution methodology, with 10 individuals in the population and 1000 iterations per evaluation.

A. Numerical Analysis for the 33-Bus Grid

Table 6 presents the results of the numerical simulations applying the proposed master-slave metaheuristic optimization methodology to the 33- bus grid compared with some reports in the literature. The comparison considered BONMIN, an MINLP solver available in the General Algebraic Modeling System (GAMS); the Chu & Beasley genetic algorithm (CBGA); the particle swarm optimizer (PSO); and the black widow optimizer (BWO).

Table 6. Comparison of results obtained for the 33-bus grid.

Method	Location (Node)	Size (Mvar)	Objective function (USD/year)	Expected reduction (%)	Processing times (s)
BONMIN	[6, 18, 30]	[0.0000, 0.1138, 0.4551]	100221.38	11.10	7.59
CBGA	[13, 30, 31]	[0.1528, 0.3227, 0.1157]	100139.21	11.18	57.6
PSO	[14, 30,31]	[0.1486, 0.3244,0.1157]	100107.24	11.21	6417.91
BWO	[14, 30, 32]	[0.1486, 0.3337, 0.1064]	100093.29	11.22	43.97
AHA	[14, 30, 32]	[0.1486, 0.3337, 0.1064]	100093.29	11.22	48.24

In light of the above, the following can be stated:

- The proposed AHA and BWO reach the best solution, with an objective function value of USD 100,093.29 per year. This value reduces the objective function by USD 11.22 compared to the benchmark case (*i.e.*, USD 112740.90) when the TSCs are placed at nodes 14, 30, and 32, with sizes of 0.1486 Mvar, 0.3337 Mvar, and 0.1064 Mvar, respectively.
- The PSO reached a solution close to that of the AHA (and the BWO) only by changing the location of a TSC from node 32 to 31. This change reduces the objective function by 11.21%.
- The CBGA reached a solution of about USD 100107.24 per year of operation, *i.e.*, a difference of about USD 45.92 with respect to the best solutions (AHA and PSO). The CGBA found a yearly reduction of about 11.18% with respect to the benchmark case. In addition, the BONMIN approach got stuck in a local optimum, which may be due to the non-convexities of the MINLP formulation.
- The results show that the BWO takes about 43.97 s to reach the solution, while the AHA takes about 48.24 s, *i.e.*, the second-best processing time.

B. Numerical Analysis for the 69-bus Grid

Table 7 presents the results of our proposal's numerical validations in the 69-bus grid, in comparison with the BWO reported by the authors of [1]. In this test feeder, the BONMIN approach fails to converge. Note that the benchmark case for the 69-bus grid corresponds to an annual operating value of about USD \$119,715.63.

These results indicate that:

- The proposed AHA achieves the same numerical result reported by the BWO, with a reduction of about 12.58% with respect to the benchmark case, *i.e.*, annual net profit of approximately USD 15057.60.
- The exact solution of the MINLP model (using the BONMIN solver) does not converge in this system, which may be due to the increased size of the solution.
- The CBGA and the PSO achieve reductions of about 12.55% and 12.56% compared to the benchmark case. These solutions can be classified as locally optimal, in contrast with those of the AHA and the BWO, which exhibit small differences.
- The AHA reports the best processing times for the 69-node grid, with about 165.60 s in solving the optimization problem studied, followed by the BWO (about 173.12 s).

Table 7. Comparison of results obtained for the 69-bus grid.

Method	Location (Node)	Size (Mvar)	Objective function (USD/year)	Expected reduction (%)	Processing times (s)
BONMIN			Does not converge		
CBGA	[21, 61, 65]	[0.0662, 0.4840, 0.0635]	104695.69	12.55	88.60
PSO	[23, 61, 64]	[0.0526, 0.4009, 0.1504]	104679.61	12.56	9325.89
BWO	[21, 61, 64]	[0.0647, 0.4363, 0.1125]	104658.03	12.58	173.12
AHA	[21, 61, 64]	[0.0647, 0.4363, 0.1125]	104658.03	12.58	165.60

The solutions provided by all optimizers indicate that node 61 is among the most sensitive to reactive power injection, with received values ranging between 400.90 kvar and 484.00 kvar. Additionally, three of the solution methods consistently identified node 21 as part of the final solution in the 69-bus grid.

5. CONCLUSIONS

This study addressed the problem regarding the optimal placement and sizing of TSCs in MVDNs while aiming to minimize annual operating costs associated with energy losses while also considering the annualized TSC investment costs. This problem was solved using a hybrid optimization methodology that combined the AHA with the successive approximations' method for power flow analysis. The

numerical results obtained in 33- and 69-bus test systems demonstrate the effectiveness of the proposed approach, which outperformed other metaheuristic algorithms such as the PSO, the CBGA, and the BWO. Specifically, the AHA exhibited superior capabilities in identifying global optima, thus achieving significant reductions in operating costs when compared to traditional approaches. Furthermore, the proposed methodology proved to be robust in terms of convergence and solution quality, making it suitable for implementation in MVDNs with topologies similar to those analyzed in this work. The AHA approach can serve as a valuable tool to plan and operate electrical systems, providing an efficient and cost-effective alternative for reactive power compensation.

Future research could investigate the application of this approach to MVDNs that incorporate renewable energy sources and variable loads. Additionally, integrating other types of FACTS could further improve network efficiency and stability.

AUTHORS' CONTRIBUTION

Dallany Giraldo-Aizales: Data curation, Conceptualization, Investigation, Methodology, Writing-original draft.

Oscar-Danilo Montoya-Giraldo: Data curation, Conceptualization, Investigation, Methodology, Writing-review, and editing.

Walter-Julián Gil-González: Conceptualization, Investigation, Methodology, Writing-review, and editing.

REFERENCES

- [1] N. Santamaria-Henao, O. D. Montoya, C. L. Trujillo-Rodríguez, "Optimal Siting and Sizing of FACTS in Distribution Networks Using the Black Widow Algorithm," *Algorithms*, vol. 16, e225, 2023. <https://doi.org/10.3390/a16050225>
- [2] E. Kabalci, "Reactive power compensation in AC power systems," in *Reactive Power Control in AC Power Systems: Fundamentals and Current Issues*, pp. 275-315, 2017. https://doi.org/10.1007/978-3-319-51118-4_10
- [3] F. O. Igbinovia, G. Fandi, J. Švec, Z. Müller, J. Tlustý, "Comparative review of reactive power compensation technologies," in *16th International Scientific Conference on Electric Power Engineering (EPE)*, 2015. <https://doi.org/10.1109/EPE.2015.7161066>
- [4] K. Pal, K. Verma, R. Gandotra, "Optimal location of FACTS devices with EVCS in power system network using PSO," *e-Prime-Advances in Electrical Engineering, Electronics and Energy*, vol. 2024, e100482, 2024. <https://doi.org/10.1016/j.prime.2024.100482>
- [5] I. M. Jawad, A. Q. Abdulrasool, A. Q. Mohammed, W. S. Majeed, H. T. H. Salim ALRikabi, "The optimal allocation of thyristor-controlled series compensators for enhancement HVAC transmission lines Iraqi super grid by using seeker optimization algorithm," *Open Engineering*, vol. 14, e20220499, 2024. <https://doi.org/10.1515/eng-2022-0499>

- [6] H. B. Tolabi, M. H. Ali, M. Rizwan, "Simultaneous reconfiguration, optimal placement of DSTATCOM, and photovoltaic array in a distribution system based on fuzzy-ACO approach," *IEEE Transactions on Sustainable Energy*, vol. 6, pp. 210-218, 2014. <https://doi.org/10.1109/TSTE.2014.2364230>
- [7] A. R. Gupta, A. Kumar, "Energy savings using D-STATCOM placement in radial distribution system," *Procedia Computer Science*, vol. 70, pp. 558-564, 2015. <https://doi.org/10.1016/j.procs.2015.10.100>
- [8] R. Sirjani, A. R. Jordehi, "Optimal placement and sizing of distribution static compensator (D-STATCOM) in electric distribution networks: A review," *Renewable and Sustainable Energy Reviews*, vol. 77, pp. 688-694, 2017. <https://doi.org/10.1016/j.rser.2017.04.035>
- [9] S. Rezaeian Marjani, V. Talavat, S. Galvani, "Optimal allocation of D-STATCOM and reconfiguration in radial distribution network using MOPSO algorithm in TOPSIS framework," *International Transactions on Electrical Energy Systems*, vol. 29, e2723, 2019. <https://doi.org/10.1002/etep.2723>
- [10] W. Gil-González, "Optimal Placement and Sizing of D-STATCOMs in Electrical Distribution Networks Using a Stochastic Mixed-Integer Convex Model," *Electronics*, vol. 12, e1565, 2023. <https://doi.org/10.3390/electronics12071565>
- [11] O. D. Montoya, W. J. Gil González, L. F. Grisales-Noreña, D. Giral, A. Molina-Cabrera, "On the optimal reconfiguration of radial AC distribution networks using an MINLP formulation: A GAMS-based approach," *Ingeniería e Investigación*, vol. 42, e91192, 2021. <https://doi.org/10.15446/ing.investig.91192>
- [12] P. Srivastava, R. Haider, V. J. Nair, V. Venkataramanan, A. M. Annaswamy, A. K. Srivastava, "Voltage regulation in distribution grids: A survey," *Annual Reviews in Control*, vol. 55, pp. 165-181, 2023. <https://doi.org/10.1016/j.arcontrol.2023.03.008>
- [13] L. F. Grisales-Noreña, B. Cortés-Caicedo, O. D. Montoya, J. C. Hernández, G. Alcalá, "A battery energy management system to improve the financial, technical, and environmental indicators of Colombian urban and rural networks," *Journal of Energy Storage*, vol. 65, e107199, 2023. <https://doi.org/10.1016/j.est.2023.107199>
- [14] K. Balamurugan, D. Srinivasan, "Review of power flow studies on distribution network with distributed generation," in *IEEE Ninth International Conference on Power Electronics and Drive Systems*, 2011. <https://doi.org/10.1109/PEDS.2011.614728>
- [15] O. D. Montoya, A. Molina-Cabrera, J. C. Hernández, "A Comparative Study on Power Flow Methods Applied to AC Distribution Networks with Single-Phase Representation," *Electronics*, vol. 10, e2573, 2021. <https://doi.org/10.3390/electronics10212573>
- [16] H. Bakır, "A novel artificial hummingbird algorithm improved by natural survivor method," *Neural Computing and Applications*, vol. 36, pp. 16873-16897, 2024. <https://doi.org/10.1007/s00521-024-09928-z>
- [17] W. Zhao, L. Wang, S. Mirjalili, "Artificial hummingbird algorithm: A new bio-inspired optimizer with its engineering applications," *Computer Methods in Applied Mechanics and Engineering*, vol. 388, e114194, 2022. <https://doi.org/10.1016/j.cma.2021.114194>
- [18] H. Bakır, "Enhanced artificial hummingbird algorithm for global optimization and engineering design problems," *Advances in Engineering Software*, vol. 194, e103671, 2024. <https://doi.org/10.1016/j.advengsoft.2024.103671>

- [19] M. Hosseinzadeh, A. M. Rahmani, F. M. Husari, O. M. Alsalami, M. Marzougui, G. N. Nguyen, S.-W. Lee, "A Survey of Artificial Hummingbird Algorithm and Its Variants: Statistical Analysis, Performance Evaluation, and Structural Reviewing," in *Archives of Computational Methods in Engineering*, 2024. <https://doi.org/10.1007/s11831-024-10135-1>
- [20] M. M. Emam, E. H. Houssein, M. A. Tolba, M. M. Zaky, M. Hamouda Ali, "Application of modified artificial hummingbird algorithm in optimal power flow and generation capacity in power networks considering renewable energy sources," *Scientific Reports*, vol. 13, 2023.
- [21] V. M. Garrido-Arévalo, W. Gil-González, O. D. Montoya, L. F. Grisales-Noreña, J. C. Hernández, "Optimal Dispatch of DERs and Battery-Based ESS in Distribution Grids While Considering Reactive Power Capabilities and Uncertainties: A Second-Order Cone Programming Formulation," *IEEE Access*, vol. 12, pp. 48497-48510, 2024.



Available in:

<https://www.redalyc.org/articulo.oa?id=413982851005>

How to cite

Complete issue

More information about this article

Journal's webpage in redalyc.org

Scientific Information System Redalyc
Diamond Open Access scientific journal network
Non-commercial open infrastructure owned by academia

Dallany Giraldo-Aizales, Oscar-Danilo Montoya-Giraldo,
Walter Gil-González

**REACTIVE POWER COMPENSATION IN MEDIUM-VOLTAGE
DISTRIBUTION NETWORKS THROUGH THYRISTOR-BASED
SWITCHED COMPENSATORS AND THE ARTIFICIAL
HUMMINGBIRD ALGORITHM
COMPENSACIÓN DE POTENCIA REACTIVA EN REDES DE
DISTRIBUCIÓN DE MEDIA TENSIÓN MEDIANTE
COMPENSADORES CONMUTADOS BASADOS EN
TIRISTORES Y EL ALGORITMO DE COLIBRÍ ARTIFICIAL
COMPENSAÇÃO DE POTÊNCIA REATIVA EM REDES DE
DISTRIBUIÇÃO DE MÉDIA TENSÃO POR MEIO DE
COMPENSADORES COMUTADOS BASEADOS EM
TIRISTORES E O ALGORITMO DO BEIJA-FLOR ARTIFICIAL**

Revista Facultad de Ingeniería

vol. 34, no. 71, e18244, 2025

Universidad Pedagógica y Tecnológica de Colombia,

ISSN: 0121-1129

ISSN-E: 2357-5328

DOI: <https://doi.org/10.19503/01211129.v34.71.2025.18244>